tributed to electron-electron[15] and electron-phonon[16] interactions. Thus any significant variation in the enhancement factor within each model would appear to indicate that these interactions are **k** dependent. The variations shown in Table V probably only reflect the uncertainty in the experimental masses. The only conclusion which we can draw with any confidence from the data listed in Table V is that the nonlocal model requires only about $\frac{3}{4}$ as much enhancement as the local model. The nonlocal model should give the more realistic value for the enhancement since the energy dependence of the matrix elements is ignored in the local model.

It is interesting to note that the local pseudopotential masses are on the whole nearly identical to the single OPW masses. Thus the average 30% enhancement found for this model indicates a 30% increase in the density of states at the Fermi level relative to the free-electron bands. The electronic specific-heat data[17] yields a value of 1.33 for the density of states relative to the free electron, which is in good agreement with our calculated average.

[15] T. M. Rice, Ann. Phys. (N. Y.) **31**, 100 (1965).
[16] N. W. Ashcroft and J. W. Wilkins, Phys. Letters **14**, 285 (1965).
[17] J. G. Duant, in *Progress in Low-Temperature Physics*, edited by C. J. Gorter (North-Holland Publishing Company, Amsterdam, 1955), p. 210.

CONCLUSIONS

A polyvalent metal such as magnesium which has Fermi surface sheets in several Brillouin zones offers a demanding test of the accuracy of any model-Hamiltonian band-structure representation. Magnesium is an element particularly suited for this test since it has a tightly bound core with a closed-shell configuration. This is the case for which the cancellation theorem should apply. The local and nonlocal pseudopotential calculations reported in this paper yield accurate models for the magnesium Fermi surface. These models should be viewed primarily as an interpolation procedure whereby one generates the entire Fermi surface from data limited to only portions of the Fermi surface. Insofar as the single-particle approximation is valid, these models also generate the entire band structure for energies other than E_F.

Comparisons of the models with the experimental data indicate that the errors in the local pseudopotential are about $\pm 3\times 10^{-3}$ Ry, while we could find no errors in the nonlocal pseudopotential model greater than our truncation error of $\pm 1.5\times 10^{-3}$ Ry. We can conclude from this that while the local pseudopotential model offers a very accurate representation of the magnesium Fermi surface, the most accurate fit to the data can only be achieved by inclusion of the nonlocal nature of the pseudopotential.

PHYSICAL REVIEW VOLUME 162, NUMBER 3 15 OCTOBER 1967

Magnetic Ordering in Dilute Solid Solutions of Iron in Gold. II. Electric Hyperfine Interactions*

C. E. VIOLET AND R. J. BORG
Lawrence Radiation Laboratory, University of California, Livermore, California
(Received 17 April 1967)

The Fe^{57} Mössbauer spectra of Au-Fe alloys with Fe concentrations between 1.7 and 10.5 at.% at temperatures between the transition temperature and room temperature consist of a doublet superimposed on a central line which is an unresolved doublet. The centroids of the two doublets are separated by 0.06±0.02 mm/sec. This is independent of Fe concentration and temperature. The outer doublet is associated with Fe ions with one or more Fe nearest neighbors, while the inner doublet is associated with Fe ions with no Fe nearest neighbors. The separation of the outer doublet lines is independent of Fe concentration and is 0.77±0.02 mm/sec at 77°K and 0.69±0.02 mm/sec at 294°K. The separation of the inner doublet is an order of magnitude smaller. It increases with increasing Fe concentration, but has no detectable dependence on temperature. These doublets are interpreted as quadrupole-split resonance lines. The electric field gradient (EFG) of the outer doublet probably arises from conduction electrons within the atomic sphere. The EFG of the inner doublet may arise from random strains, or Fe impurity charges beyond the nearest-neighbor shell, or both. An analysis of the temperature shifts gives an effective Debye temperature of (290±40)°K for Fe impurities in Au. The observed linewidths are independent of Fe concentration and temperature from 77 to 294°K. The linewidths increase slightly at a few degrees above the transition temperature, perhaps because of the onset of magnetic-relaxation effects.

I. INTRODUCTION

IN a previous paper[1] (henceforth called VB-1) we presented the results of an investigation in which the Mössbauer effect was used to observe magnetic ordering in dilute solid solutions of Fe in Au. The magnitude of the hyperfine splitting was studied as a function of composition and temperature, and the magnetic transition temperature (T_0) was determined as a function of composition. Spectra were obtained for

* Work performed under the auspices of the U. S. Atomic Energy Commission.
[1] C. E. Violet and R. J. Borg, Phys. Rev. **149**, 540 (1966).

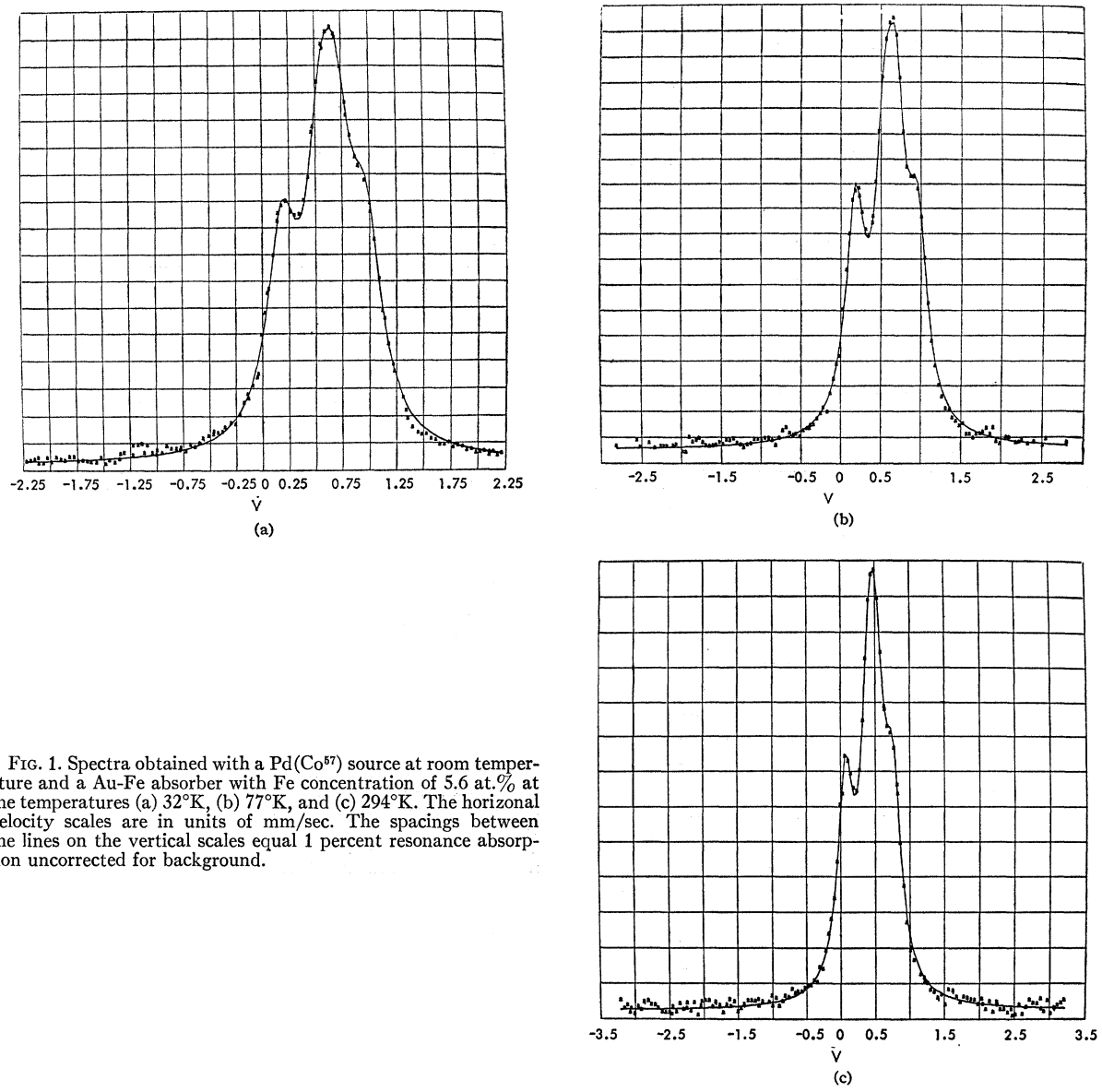

FIG. 1. Spectra obtained with a Pd(Co^{57}) source at room temperature and a Au-Fe absorber with Fe concentration of 5.6 at.% at the temperatures (a) 32°K, (b) 77°K, and (c) 294°K. The horizonal velocity scales are in units of mm/sec. The spacings between the lines on the vertical scales equal 1 percent resonance absorption uncorrected for background.

alloys ranging in composition from 0.84 to 7.4 at.% Fe, all of which demonstrate rather sharp transitions from the paramagnetic to the ordered state. In this paper we will turn aside from the magnetically ordered state to present an analysis of the data obtained in the paramagnetic region.[2]

Three classes of spectra were defined in VB-1 on the basis of their appearance: class I spectra are those which exhibit a well-defined, six-line Fe^{57} hyperfine spectrum; class II denotes the collapsed spectrum which occurs just below the transition temperature; and class III spectra are obtained at temperatures above the transition temperature. Thus, it is the analysis of class III spectra with which this report is concerned. These spectra do not demonstrate a single sharp Lorentzian line but instead the complex spectra illustrated in Figs. 1 and 2. The main features of interest are the slow but definite development, with increasing concentration of Fe, of two subsidiary peaks on the wings of the central peak. This gives the appearance of two outer lines superimposed on a single central line. Our results show that the central line is associated only with "isolated Fe," i.e., Fe ions which have no Fe nearest neighbors while the outer lines are a quadrupole split line associated with "neighboring Fe," i.e., Fe ions with one or more Fe nearest neighbors.

II. EXPERIMENTAL

A detailed description of the experimental procedure is given in VB-1. Suffice it to say that all specimens were

[2] The paramagnetic region in this experiment is between T' and 294°K, where T' is a few degrees above T_0.

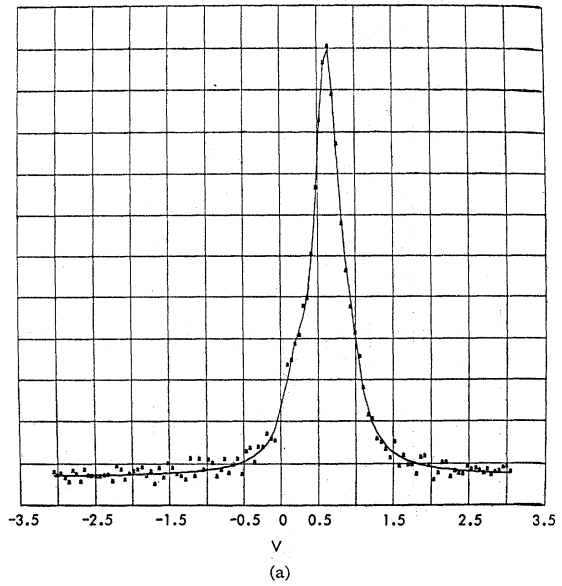

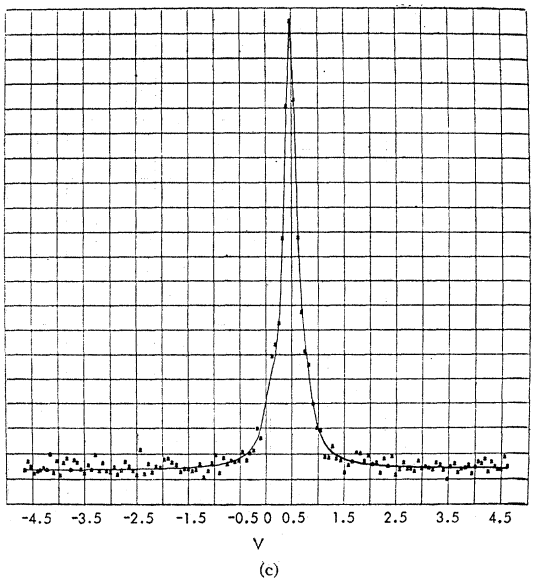

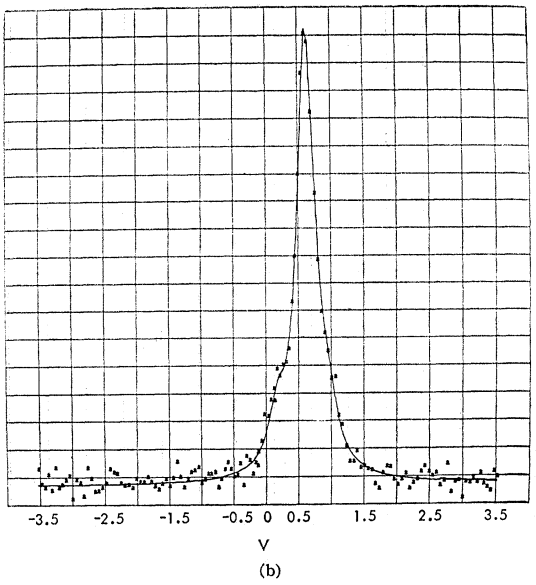

FIG. 2. Spectra obtained from a Pd(Co^{57}) source at room temperture and a Au-Fe absorber with Fe concentration of 1.7 at.% at the temperature (a) 17°K, (b) 77°K, and (c) 294°K. The horizonal velocity scales are in units of mm/sec. The spacings between the lines on the vertical scale are (a) 1 percent, (b) and (c) 0.5 percent resonance absorption uncorrected for background.

prepared as absorbers containing Fe enriched in Fe^{57}, with the exception of AuS-8 which was a source. The Fe concentrations (x) and magnetic transition temperatures (T_0) for the specimens examined in this paper are given in Table I. These data differ from Table II of VB-1 in the following respects: (1) the Fe concentration of sample Au-Fe 7 has been adjusted from 6.7 to 5.6 at.% Fe; (2) data from two additional samples, AuS-8 and Au-Fe 1a, are included; (3) the most dilute alloys of VB-1, AuS-5 and Au-Fe 2, are excluded since their class III spectra showed no detectable structure.

The Fe concentrations were previously[1] determined by spectrographic analysis to an accuracy of ±10%. We have subsequently redetermined all compositions by x-ray fluorescence which is accurate to ±3%. Only sample Au-Fe 7 was outside the limits of error of the

TABLE I. Au-Fe samples and results.

Sample	Au-Fe 9	Au-Fe 11	Au-Fe 8	Au-Fe 7	AuS-8	Au-Fe 1a
Fe concentration (at.%)	1.7	2.9	4.4	5.6	8.0	10.5
Transition temperature (°K)	14.8±0.5	17±1	23.5±0.5	27.6±0.5	31±2	40±2
$\langle a_1/a_0\rangle_T$	0.23±0.04	0.41±0.05	0.58±0.09	0.83±0.08	1.74±0.20	3.03±0.20
$2\epsilon_{34}$(mm/sec)	0.05±0.03	0.13±0.03	0.11±0.02	0.14±0.02	0.19±0.03	0.07±0.07

TABLE II. Line separations of outer doublet.[a]

Temp. (°K)	T' (see Table III)	77°K	294°K
$2\epsilon_{12}$(mm/sec)	0.78±0.02	0.77±0.02	0.69±0.02

[a] The average of all compositions.

x-ray fluorescence method. There is no systematic difference in the two methods of analysis[3] and this change has no significant effect on the results of VB-1.

III. ANALYSIS OF THE DATA

Initially, an equation composed of the sum of three Lorentzians was fitted by an IBM 7094 computer to all spectra by a least squares analysis. The linewidths and all other parameter were allowed to vary independently. In all cases the width of the central line was significantly larger than the linewidths of the two outer lines which were essentially equal to each other. This suggests that either some mechanism of line broadening (e.g., magnetic relaxation)[4] is operative for the central line and not for the two outer lines, or the central line is a composite of two or more lines. Either of these alternatives implies a non-Lorentzian shape for the central line.

To examine the question of the central-line shape as well as to obtain a measure of its broadening, we represent the central line as a closely spaced doublet.[5] The spectra then consists of an inner doublet and an outer doublet and can be described by the equation

$$A(v)=A(\infty)+A_1\left\{\left[\frac{2}{\Gamma_1}(v-(v_{12}-\epsilon_{12}))\right]^2+1\right\}^{-1}+A_2\left\{\left[\frac{2}{\Gamma_2}(v-(v_{12}+\epsilon_{12}))\right]^2+1\right\}^{-1}$$
$$+A_3\left\{\left[\frac{2}{\Gamma_3}(v-(v_{34}-\epsilon_{34}))\right]^2+1\right\}^{-1}+A_4\left\{\left[\frac{2}{\Gamma_4}(v-(v_{34}-\epsilon_{34}))\right]^2+1\right\}^{-1}, \quad (1)$$

where $A(v)$=absorption for velocity v, $A(\infty)$=absorption for a velocity large enough for any resonance process to be negligible, A_1,A_2=the maximum absorption of the outer doublet lines, A_3,A_4=the maximum absorption of the inner doublet lines, $\Gamma_{1,2}$=linewidths of the outer doublet, $\Gamma_{3,4}$=linewidths of the inner doublet, v_{12}=the center shift of the outer doublet, and v_{34}=the center shift of the inner doublet.

Equation (1) was fitted to all spectra by least squares with the constraint that all linewidths be equal ($\Gamma_1=\Gamma_2=\Gamma_3=\Gamma_4=\Gamma_0$). This results in the determination of ten parameters, which equals the number of adjustable parameters in the unconstrained three-Lorentzian equation. In every case the average sum of the squared residuals was significantly smaller for Eq. (1) constrained than for the three-Lorentzian equation unconstrained. Also, with Eq. (1) the linewidths of the outer doublet, Γ_1 and Γ_2, were nearly the same as for the three-Lorentzian unconstrained fits. Since the unconstrained three-Lorentzian and the constrained four-Lorentzian equations have the same number of adjustable parameters, we assume the latter (Eq. 1), which consistently gives significantly better fits to the data, is the better approximation. We conclude that the shape of the outer doublet lines are Lorentzian within experimental error and the shape of the central line is non-Lorentzian and broadened relative to the outer lines.

The values of the parameters resulting from fitting Eq. (1) to all spectra are presented and discussed in the following sections. The parameters were examined for any significant dependence on temperature or Fe concentration. In cases where no dependence on temperature (T) or Fe concentration (x) exists, the values are averaged over T or x. Such averaged values are symbolized as $\langle\rangle_T$ or $\langle\rangle_x$. The ranges over which these averages are calculated are $T'\leq T\leq 294$°K and $0.017\leq x\leq 0.105$ (where x is the mole fraction of Fe). The errors assigned to the experimentally desired quantities are rms errors.

IV. DISCUSSION OF PARAMETERS

A. Line Intensity Ratios

The class III spectra have the following features:[1] (1) The intensity ratio and separation of the two outer lines do not vary appreciably with the concentration of Fe and their intensities increase relative to the central line with increasing Fe concentration; and (2) the centroid of the two outer lines is shifted relative to that of the central line for the T and x ranges of this experiment. These features suggest that: (1) The two outer lines are a quadrupole split resonance line and (2) the central line and the two outer lines appear to be associated with Fe nuclei in two states which are well defined in terms of their electric hyperfine interactions (electric monopole, i.e., isomer shift, and electric quadrupole).

To interpret the observed line intensities we postulate the following: (1) The central line is associated only with "isolated Fe," i.e., Fe ions with no Fe nearest neighbor, while the two outer lines are associated only with "neighboring Fe," i.e., Fe ions which have one or

[3] For example: [x(*Au-Fe* 7)/x(*Au-Fe* 9)] (x-ray fluorescence) =3.3, [x(*Au-Fe* 7)/x(*Au-Fe* 9)] (spectrography)=(6.7/1.7±$\sqrt{2}$ ×10%=3.9±0.6. The deviation of the spectrographic ratio from the x-ray fluorescence ratio is only one standard error. Therefore the spectrographic method is completely consistent with the x-ray fluorescence method.

[4] F. van der Woude and A. J. Dekker, Phys. Status Solidi 9, 775 (1965).

[5] The central line could as well be represented as the sum of three or more Lorentzians. However, these more complex representations do not appear to be necessary to interpret our results.

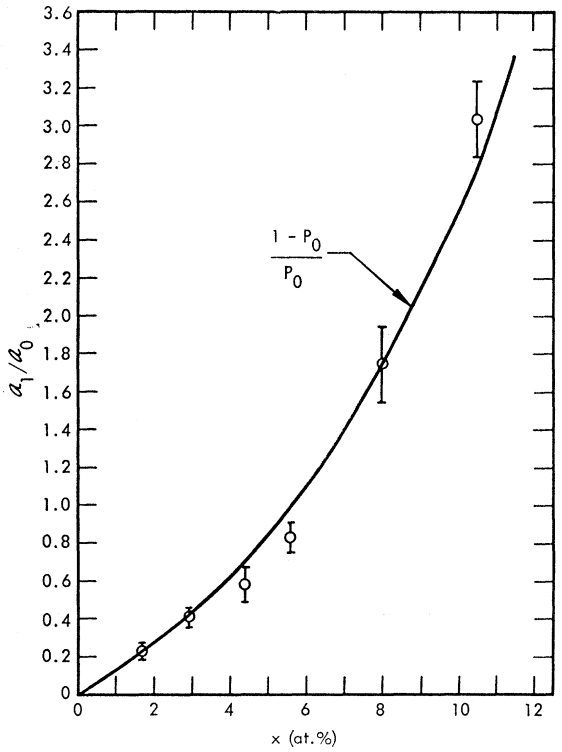

FIG. 3. The measured ratio of the outer line intensity, a_1, to the central line intensity, a_0, plotted against Fe concentration.

more Fe nearest neighbors; and (2) the alloys are solid solutions.[6]

If a_0 and a_1 are the areas under the central line and the two outer lines, respectively, then from these postulates

$$\frac{a_1}{a_0}=\frac{1-(1-x)^{12}}{(1-x)^{12}}, \tag{2}$$

where x is the mole fraction of Fe. The measured values of a_1/a_0 are independent of temperature within experimental error for all compositions. These ratios averaged over temperature, $\langle a_1/a_0\rangle_T$, are given in Table I. They are also plotted and compared with Eq. (2) in Fig. 3. The excellent agreement between the experimental points and Eq. (2) constitutes experimental verification both of the above postulates.

B. Line Separations

The separations of the two outer lines $2\epsilon_{12}$ are independent of Fe concentration within experimental error. In fact, all of the energy-dependent parameters associated with the outer lines, $2\epsilon_{12}$, v_{12}, and Γ_0 are independent of Fe concentration (see sections C, D and E). The line separations $2\epsilon_{12}$ exhibit a small but significant dependence on temperature. Values of $2\epsilon_{12}$ averaged over the Fe concentration $\langle 2\epsilon_{12}\rangle_x$ for the temperatures T', and 294°K, appear in Table II. The temperatures T' of the various samples are from 1 to 10°C above the sample transition temperatures T_0. The separations of the inner lines $2\epsilon_{34}$ are independent of temperature within experimental error but generally increase with increasing Fe concentration. Values of $2\epsilon_{34}$ averaged over temperature are given in Table I and plotted in Fig. 4.

With respect to the incremental width of the central line (of which $2\epsilon_{34}$ is a measure) we make the following observations: If the spin-spin mechanism were operative one would expect the relaxation to "speed up" as the Fe concentration increases and linewidths to decrease correspondingly. However, the incremental linewidth of the central line increases with increasing Fe concentration. Therefore, spin-spin relaxation does not appear to be associated with the central line.

If the spin-lattice mechanism were operative, one would expect the relaxation to "speed up" with increasing temperature with a corresponding decrease in the central linewidth. However, $2\epsilon_{34}$ has no detectable dependence on temperature between 77 and 294°K. Therefore, spin-lattice relaxation does not appear to be associated with the central line. We postulate that the central line is not a broadened single resonance line but rather a quadrupole-split resonance line.

Electric field gradients at nuclei in metals can be expressed as[7]

$$q=q_{\text{latt}}(1-\gamma_\infty)+q_{\text{loc}}(1-R_Q),$$

where q_{loc}=field gradient due to conduction electrons within the atomic sphere,[8] q_{latt}=field gradient due to lattice charges, i.e., charges outside the atomic sphere, and γ_∞,R_Q=Sternheimer factors.[7] Calculations show that in general q_{loc} is at least an order of magnitude, greater than q_{latt}. This combined with the fact that $2\epsilon_{12}$ is about one order of magnitude greater than $2\epsilon_{34}$

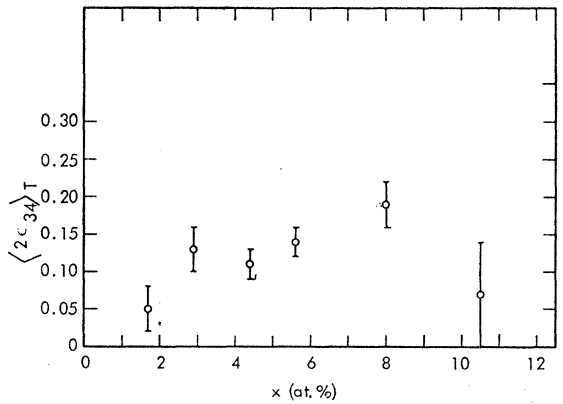

FIG. 4. The splitting of the central line, $\langle 2\epsilon_{34}\rangle_T$ in mm/sec, plotted against the Fe concentration.

[6] For a random distribution of Fe ions in the fcc Au lattice the probabilities of 0, 1, 2, and 3 nearest neighbors are approximately, 24, 37, 26, and 10%, respectively, for x=10.5 at.%.

[7] R. E. Watson, A. C. Gossard, and Y. Yafet, Phys. Rev. **140**, A375 (1965).

[8] The atomic spheres are centered at lattice points with a radius such that nearest neighbors spheres are tangent to each other (see Ref. 7).

TABLE III. Center shifts and excess linewidths.

	Samples					Average for all samples	
x(at.%)	1.7	2.9	5.6	8.0	10.5		
T'(°K)	17	18	32	40	45	77°K	294°K
$\Delta\Gamma_0$[a](mm/sec)	0.10	0.09	0.05	0.10	0.09	0.03	0.01
v_{34}(mm/sec)	0.62±0.01	0.62±0.01	0.62±0.01	0.57±0.02	0.59±0.02	0.61±0.01	0.45±0.01
v_{12}(mm/sec)	0.56±0.01	0.56±0.01	0.57±0.01	0.56±0.01	0.55±0.01	0.56±0.01	0.40±0.01

[a] The rms error in $\Delta\Gamma_0$ is ±0.04 mm/sec.

suggests that $q_{\text{loc}} \gg q_{\text{latt}}$ for the "neighboring Fe" while the reverse is true for the "isolated Fe". In the latter case the sources of q_{latt} could be either random strains in the lattice or the Fe impurity charges beyond the nearest neighbor shell, or both.

The decrease in $2\epsilon_{12}$ as the temperature increases from 77 to 294°K is too large to be accounted for by the thermal variation of the lattice constant. This decrease may be a result of thermal-repopulation effects across the Fermi energy.[7]

The magnetic hyperfine spectra of these alloys show detectable quadrupole effects only for those alloys containing 5.6 at.% Fe, or more.[1] This suggests that (1) In the magnetically ordered state, $q_{\text{loc}} \ll q_{\text{latt}}$ for *all* Fe nuclei, (2) All Fe ions in the magnetically ordered state have the same conduction electron configuration as the "isolated Fe" ions in the paramagnetic state, and (3) the sources of q_{latt} for the magnetically ordered state are the same as for the paramagnetic state, i.e., random strains or Fe impurity charges, or both.

C. Peak Intensity Ratios

The peak intensity ratios of the outer doublet and inner doublet, (A_2/A_1) and (A_3/A_4), respectively, are independent of both temperature and Fe concentration within experimental error. Averaged over both temperature and Fe concentration, $\langle\langle A_2/A_1\rangle_T\rangle_x$ and $\langle\langle A_3/A_4\rangle_T\rangle_x$ yield 1.10±0.02 and 1.02±0.02 for their respective values. The peak intensities of the outer doublet lines are unequal. This is consistent with our assumption that the outer lines are a quadrupole doublet associated with the "neighboring Fe." The asymmetry in the force constants resulting from the bonding to both the Fe and the Au nearest neighbors would be expected to increase the anisotropy of the Debye-Waller factor. This can result in unequal intensities of the observed quadrupole doublet lines.[9]

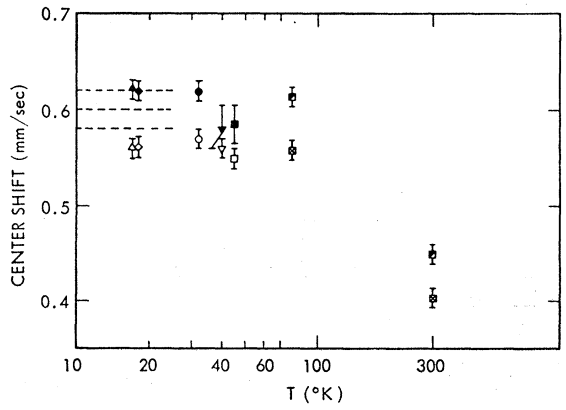

FIG. 5. The center shifts of the outer lines, v_{12}, and central line, v_{34}, plotted against temperature. Δ—1.7 at.%, ◇—2.9 at.%, ○—5.6 at.%, ▽—8.0 at.%, □—10.5 at.%, ◩—average of all samples.

The peak intensities of the inner doublet are equal. Assuming the inner doublet is also a quadrupole split resonance line, this would be expected if the central line is associated with the "isolated Fe." The bonding to the 12 Au nearest neighbors is nearly isotropic and no asymmetry in the quadrupole lines is observed.

D. Observed Linewidth

For all samples, the observed linewidth Γ_0 is significantly larger at T' than at 77°K or 294°K. We define an "excess linewidth" $\Delta\Gamma_0 = \Gamma_0 - \Gamma_0(\text{calc})$ where $\Gamma_0(\text{calc}) = 0.23(1+0.135t)$.[1] The effective absorber thickness, t, for each sample was obtained from the maximum resonance absorption A_m by way of the well-known equation that relates these quantities; $A_m = f_s[1 - I_0(t/2)\exp(-t/2)]$. A_m(corrected for background) is obtained from: $A_m = A_1 + A_2 + A_3 + A_4$ (see Eq. 1) and $f_s = 0.65$.[1]

The values of $\Delta\Gamma_0$ are given in Table III and plotted in Fig. 5. At 77 and 294°K the $\Delta\Gamma_0$'s for all samples are equal within experimental error. Therefore, average values $\langle\Delta\Gamma_0\rangle_x$ are plotted at these temperatures. For 77 and 294°K the values of $\langle\Delta\Gamma_0\rangle_x$ are nearly zero. However, at the temperatures, T', the $\Delta\Gamma_0$'s are significantly greater than zero. This line broadening probably results from magnetic relaxation.[4] This can occur when, as the temperature of the paramagnet is reduced, the Fe ion spin-flipping frequency becomes comparable to the nuclear Larmor frequency.[4] This broadening may also be associated with some persistent short-range magnetic order which exists above T_0.

The fact that Γ_0 has no explicit dependence on Fe concentration indicates that the two outer lines are not each composits of two or more resonance lines. They are each single resonance lines.

E. Center Shifts

The center shifts, v_{12} and v_{34}, are given in Table III and plotted in Fig. 6. The isomer shift and the second-

[9] V. I. Gol'danskii, E. F. Markarov, and V. V. Khrapov, Zh. Eksperim i Teor. Fiz. 44, 752 (1963) [English transl.: Soviet Phys.—JETP 17, 508 (1963)].

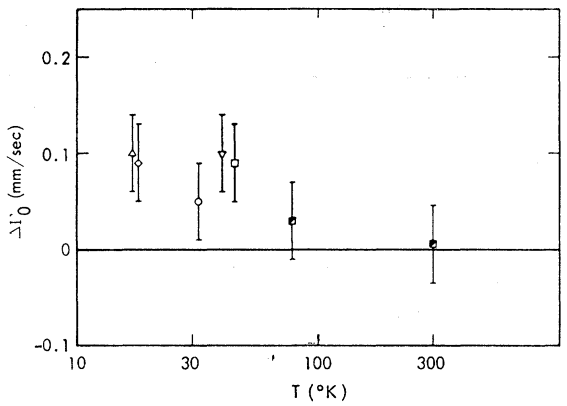

FIG. 6. The "excess linewidth," $\Delta\Gamma_0$, plotted against temperature. ▲—v_{34}, Δ—v_{12} for 1.7 at.%, ♦—v_{34}, ◇—v_{12} for 2.9 at.% ●—v_{34}, ○—v_{12} for 5.6 at.%, ▼—v_{34}, ▽—v_{12} for 8.0 at.% ■—v_{34}, □—v_{12} for 10.5 at.%, ◩—v_{34} average of all samples ⊠—v_{12} average of all samples.

order Doppler shift both can contribute to the center shift. The variation of the second-order Doppler shift for our values of T' is certainly negligible. Therefore, differences in center shift of these samples at T' are essentially differences in the isomer shift. At 77 and 294°K, the v_{12}'s of all samples are the same within experimental error and hence the average value $\langle v_{12}\rangle_x$ is given at these temperatures. The same is true for v_{34} and the average value $\langle v_{34}\rangle_x$ is also given at these temperatures.

The center shifts of the magnetic hyperfine (class I) spectra of these samples are independent of both temperature and Fe concentration.[1] Therefore, in VB-1 we have quoted this as an isomer shift averaged over T and x for $2.2°K \leq T \leq 25°K$ and $(0.008 \leq x \leq 0.08)$;

$$\langle\langle\delta\rangle_T\rangle_x = +(0.60\pm0.02)\ \text{mm/sec}$$

relative to a Pd source at 294°K.[10] This value is plotted in Fig. 6 up to 25°K, the highest temperature at which it was measured. We can now determine whether the isomer shifts of the class III spectra differ from the isomer shift of the class I spectra. Using the shifts for Au-Fe 9 at 17°K and Au-Fe 11 at 18°K (Table III), we have for the differences in shifts

$$v_{34}-\langle\langle\delta\rangle_T\rangle_x = +(0.02\pm0.02)\text{mm/sec},$$

$$v_{12}-\langle\langle\delta\rangle_T\rangle_x = -(0.04\pm0.02)\text{mm/sec, for } T\leq 25°K.$$

The isomer shift of the central line (c_{34}) differs from $\langle\langle\delta\rangle_T\rangle_x$ by one rms error and hence this difference is not significant. However, the isomer shift of the outer doublet (v_{12}) is definitely less than $\langle\langle\delta\rangle_T\rangle_x$ and perforce v_{34}. These results as well as the quadrupole effects discussed in (B) suggest that the Fe ions in the magnetically ordered state have the same conduction electron configuration as the "isolated Fe" ions in the paramagnetic state.

[10] To quote isomer shifts relative to an Fe source at 294°K, add 0.20 mm/sec to the values obtained with a Pd source at 294°K.

The difference between v_{12} and v_{34} is independent of T and x within experimental error. Its value averaged over T and x is

$$\langle\langle v_{34}-v_{12}\rangle_T\rangle_x = +(0.06\pm0.02)\text{mm/sec}.$$

The sign of this number demonstrates that the electron density at the nucleus of the "neighboring Fe" is greater than that of the "isolated Fe."

The temperature shifts of both v_{12} and v_{34} for all samples have been fitted by least squares to the following equation[11]:

$$v(T)=v(0)+\frac{9kT}{2mc}\left(\frac{T}{\Theta_e}\right)^3\int_0^{\Theta_e/T}\frac{x^3}{e^x-1}dx$$

(where the symbols have their conventional meanings) and the best values of the effective Debye temperature, Θ_e, were obtained.

No detectable correlation exists between Θ_e and v_{12} or v_{34}. Therefore the effective Debye temperature averaged over all the data is $\Theta_e=(290\pm40)°K$. This agrees with the well-known equation for the effective Debye temperature of an impurity[11]

$$\Theta_e(M_{\text{host}}/M_{\text{imp}})^{1/2}\Theta_{\text{host}}.$$

In Au-Fe alloys this equation gives

$$\Theta_e=308°K.$$

V. CONCLUSIONS

In our Au-Fe alloys with Fe concentrations up to 10.5 at.%, the Fe ions are distributed randomly in the fcc Au lattice, i.e., these alloys are true solid solutions. The electric monopole and quadrupole hyperfine interactions which are inferred from the Fe^{57} Mössbauer spectra indicate that the Fe ions, despite their random distribution in these alloys, have just two kinds of electronic configurations. One configuration is associated with "isolated Fe," i.e., Fe ions with no Fe nearest neighbors. The other is associated with "neighboring Fe," i.e., Fe ions with one or more Fe nearest neighbors. A well-defined electric field gradient (EFG) is inferred at the nuclei of the "neighboring Fe." It's primary source is probably the conduction electrons within the atomic sphere. An EFG is also inferred at the nuclei of the "isolated Fe." This is an order of magnitude less than that of the "neighboring Fe." It probably arises from random strains or the Fe impurity charges beyond the nearest-neighbor shell or both. Based on the isomer shifts and quadrupole effects that are observed in magnetically ordered and the paramagnetic states, it appears that the conduction electron configuration of *all* Fe ions in the magnetically ordered

[11] J. P. Schiffer, P. N. Parks, and J. Herberle, Phys. Rev. 133. A1553 (1964).

state is the same as that of the "isolated Fe" in the paramagnetic state. This implies that a change occurs in the conduction electron configuration of the "neighboring Fe" across the magnetic transition temperature.

ACKNOWLEDGMENTS

We wish to thank Don Freeman for developing the least squares fitting program, and R. Gutmacher for the x-ray fluorescence analysis.

PHYSICAL REVIEW VOLUME 162, NUMBER 3 15 OCTOBER 1967

Optical Properties of Vacuum-Evaporated White Tin*

R. A. MacRae† and E. T. Arakawa
Health Physics Division, Oak Ridge National Laboratory, Oak Ridge, Tennessee

and

M. W. Williams‡
Physics Department, University of Tennessee, Knoxville, Tennessee

(Received 5 January 1967; revised manuscript received 19 April 1967)

Near-normal incidence-reflectance data on vacuum-evaporated white tin films, produced *in situ*, are presented for incident photon energies from 2.1 to 14.5 eV. In addition, the real part of the refractive index has been measured from 14.5 to 20.5 eV by the critical-angle method. These results are combined with previously published data for white tin films and an analysis of optical data is carried out from 0.1 to 27.5 eV. Separation of the dielectric constants into contributions due to free and bound electrons indicates interband transitions at 1.2±0.1 and 24.5±0.1 eV, as found by previous workers, and a further interband transition at approximately 3 eV. Tentative identification of these transitions is made using published energy-band calculations. The energy-loss functions for surface and volume plasmons show sharp peaks at 9.2 and 13.4 eV, respectively, in agreement with electron-energy-loss measurements. Sum rules are used to interpret the effective number of electrons per atom at various incident photon energies.

I. INTRODUCTION

THERE is very little data in the literature on the optical constants of white tin[1–8] and no comprehensive analysis of optical data over an extensive energy range. This paper presents an analysis of the real and imaginary parts, $n(E)$ and $k(E)$, respectively, of the energy-dependent complex refractive index over the energy range 0.1 to 27.5 eV. In order to do this, measurements of optical constants have been made in the energy ranges where insufficient data are available in the literature. The quantities $n(E)$ and $k(E)$ are used to calculate the real and imaginary parts, $\epsilon_1(E)$ and $\epsilon_2(E)$, respectively, of the complex dielectric constant $\epsilon(E)$ and also the energy-loss functions, $-\mathrm{Im}[1/(\epsilon+1)]$ for surface plasmons and $-\mathrm{Im}(1/\epsilon)$ for volume plasmons. Some discussion and interpretation of these quantities are presented in terms of free-electron-like behavior, interband transitions, and collective oscillations. The interband transitions found in the present analysis are compared with the available band-structure calculations for white tin. In addition, the energy-loss functions are compared with published electron-energy-loss data.

* Research sponsored by the U. S. Atomic Energy Commission under contract with Union Carbide Corporation.

† Consultant, Oak Ridge National Laboratory; Jacksonville State University, Jacksonville, Alabama.

‡ Consultant, Oak Ridge National Laboratory.

[1] Landolt-Börnstein, *Zahlenwerte und Funktionen II* (Springer-Verlag, Berlin, 1962) Vol. 8, p. 15.

[2] J. N. Hodgson, Proc. Phys. Soc. (London) **B68**, 593 (1955).

[3] W. C. Walker, O. P. Rustgi, and G. L. Weissler, J. Opt. Soc. Am. **49**, 471 (1959).

[4] A. I. Golovashkin and G. P. Motulevich, Zh. Eksperim. i Teor. Fiz. **47**, 64 (1964) [English transl.: Soviet Phys.—JETP **20**, 44 (1965)].

[5] K. Codling, R. P. Madden, W. R. Hunter, and D. W. Angel, J. Opt. Soc. Am. **56**, 189 (1966).

[6] W. R. Hunter, *Optical Properties and Electronic Structure of Metals and Alloys*, edited by F. Abelès (North-Holland Publishing Company, Amsterdam, 1966), p. 136.

[7] R. A. MacRae, E. T. Arakawa, and R. N. Hamm, J. Opt. Soc. Am. **56**, A550 (1966).

[8] A. P. Lenham and D. M. Treherne, J. Opt. Soc. Am. **56**, 752 (1966).

II. SURVEY OF PREVIOUS OPTICAL DATA

Optical constants for tin in the energy range 0.1 to 1.3 eV have been determined by Hodgson[2] and by Golovashkin and Motulevich.[4] Both used evaporated tin films which were prepared outside, and then transferred into, the reflectometer. The change in polarization of radiation reflected from these films was analyzed to give $n(E)$ and $k(E)$. There is fair agreement between the values of $n(E)$ and $k(E)$ contained in these two references. However, the data of Golovashkin and Motulevich are more extensive and contain less scatter than that of Hodgson. Lenham and Treherne[8] have determined $\epsilon_1(E)$ and $\epsilon_2(E)$ for the principal directions in crystalline tin from below 0.1 to 3.1 eV. However, it is found that the values of $n(E)$ and $k(E)$ calculated